

# Diabetes and radiocontrast media increase endothelin converting enzyme-1 in the kidney

M Khamaisi<sup>1,2</sup>, I Raz<sup>1,2</sup>, V Shilo<sup>2</sup>, A Shina<sup>3</sup>, C Rosenberger<sup>4</sup>, R Dahan<sup>2</sup>, Z Abassi<sup>5</sup>, R Meidan<sup>6</sup>, S Lecht<sup>7</sup> and SN Heyman<sup>3</sup>

<sup>1</sup>Department of Medicine, Hadassah Hospital, Ein Kerem, The Hebrew University Medical School, Jerusalem, Israel; <sup>2</sup>Diabetes Research Unit, Department of Medicine, Hadassah Hospital, Ein Kerem, The Hebrew University Medical School, Jerusalem, Israel; <sup>3</sup>Department of Medicine, Hadassah Hospital, Mt Scopus, The Hebrew University Medical School, Jerusalem, Israel; <sup>4</sup>Department of Nephrology and Medical Intensive Care, Charité University Clinic, Berlin, Germany; <sup>5</sup>Department of Physiology, Faculty of Medicine, Technion, Haifa, Israel; <sup>6</sup>Department of Animal Sciences, Faculty of Agricultural, Food and Environmental Quality Sciences, The Hebrew University of Jerusalem, Rehovot, Israel and <sup>7</sup>Department of Pharmacology and Experimental Therapeutics, School of Pharmacy, Faculty of Medicine, The Hebrew University of Jerusalem, Jerusalem, Israel

Plasma endothelin-1 levels rise in diabetes and after exposure to contrast media suggesting a role in progressive diabetic and acute radiocontrast nephropathies. Here we studied individual and combined effects of streptozotocin-induced diabetes and contrast media on renal endothelin converting enzyme-1 levels in the rat. *In vivo*, medullary (but not cortical) endothelin converting enzyme protein gradually increased 4 to 5-fold following the induction of diabetes or after the administration of contrast media but rose 15-fold when diabetic rats were given contrast media. Changes in mRNA expression paralleled those of the protein. Immunohistochemistry confirmed that increased tubular and endothelial cell endothelin converting enzyme-1 were most pronounced in the medulla. *In vitro*, endothelin-1 levels increased 3-fold following incubation of endothelial cells with media high in glucose or with contrast and 4-fold with their combination. Endothelin converting enzyme-1 protein and mRNA expression changed in a similar pattern while prepro endothelin-1 mRNA increased with each insult but not in an additive way. Our study shows that diabetes and contrast media up-regulate renal medullary endothelin converting enzyme-1 expression and synthesis.

*Kidney International* (2008) **74**, 91–100; doi:10.1038/ki.2008.112; published online 2 April 2008

KEYWORDS: diabetes; rat; kidney; hypoxia; contrast media

Early experimental diabetes is associated with reduced renal parenchymal oxygenation that is most prominent in the renal medulla,<sup>1–3</sup> a region already functioning at low oxygen tension under normal physiologic conditions.<sup>4</sup> The decline in renal parenchymal pO<sub>2</sub> predominantly reflects enhanced tubular transport, the consequence of increased glomerular filtration rate and solute delivery to the distal nephron, as well as to augmented tubular mass and sodium transporters.<sup>1,3,5</sup> A role for altered renal hemodynamics in diabetes-associated renal hypoxia has not been clearly defined so far,<sup>6–8</sup> but remains a possibility, as important regulators of renal vascular tone are altered, such as nitrovasodilation<sup>9</sup> and ambient adenosine concentration.<sup>10</sup> Distorted anatomy of the renal microcirculation, related to diabetic glomerulopathy, may also play an important role in advanced disease.<sup>11</sup>

Reduced renal oxygenation in the diabetic kidney is associated with cellular hypoxia-adaptive response, mediated in part through hypoxia-inducible factors.<sup>3</sup> Diabetes predisposes to radiocontrast-induced nephropathy (CIN), a common cause of acute renal failure.<sup>12–14</sup> At any given degree of baseline glomerular filtration rate, diabetes doubles the risk of developing CIN as compared with nondiabetic patients.<sup>15</sup> The administration of iodinated radiocontrast media (CM) acutely reduces renal parenchymal oxygenation<sup>16</sup> in a distribution pattern similar to that of diabetes-related chronic hypoxia.<sup>17</sup> As with diabetes, CM-induced medullary hypoxia, reflecting enhanced oxygen consumption for tubular transport, combined with altered regional hemodynamics, is associated with hypoxia-inducible factor response and is believed to play a central role in the pathogenesis of CIN.<sup>18</sup>

Both diabetes<sup>19,20</sup> and the administration of CM<sup>16</sup> are associated with enhanced endothelin-1 (ET-1) production. As ET-1 markedly affects renal hemodynamics and tubular transport through specific endothelin ET<sub>A</sub> and ET<sub>B</sub> receptors,<sup>21</sup> it is conceivable that it plays an important role in the changes in renal parenchymal microcirculation and

**Correspondence:** M Khamaisi, Department of Internal Medicine B, Hadassah University Hospital, Ein Kerem, PO Box 12000, Jerusalem 91240, Israel. E-mail: [murir@hadassah.org.il](mailto:murir@hadassah.org.il)

Received 20 August 2007; revised 4 January 2008; accepted 30 January 2008; published online 2 April 2008

oxygenation observed in the diabetic kidney, and particularly following the administration of CM.<sup>22</sup>

The biologically active endothelins are produced by sequential proteolysis of the precursor prepro-endothelins. The intermediate peptide, big endothelin undergoes a final proteolysis by ubiquitous endothelin-converting enzyme (ECE) isoforms.<sup>23,24</sup> The role of these enzymes in the determination of the rate of endothelin synthesis remains to a large extent unknown. We hypothesized that the major isoform ECE-1 may play a key role in the rising circulating and renal endothelin levels found in diabetes and after the exposure to CM.

To test this assumption, we explored the independent and combined effects of diabetes and CM on ECE-1 synthesis and content in the rat renal parenchyma. Because endothelin ET<sub>B</sub> upregulation was found in the renal medulla in rats with congestive heart failure<sup>25</sup> and chronic tubulointerstitial disease,<sup>26</sup> presumably compensating for intensified ambient hypoxemia, we also looked for endothelin ET<sub>B</sub> receptor upregulation in diabetic kidneys. To isolate the independent effects of hyperglycemic environment and radiocontrast medium upon ECE-1 synthesis, in additional experiments we studied the effect of hyperglycemia and CM on ET-1, prepro-ET-1, and ECE-1 expression in cultured endothelial cells.

## RESULTS

### Induction of diabetes and the impact of CM

Streptozotocin (STZ)-induced diabetic rats developed hyperglycemia ( $401 \pm 9$  mg per 100 ml within 48 h, as compared with  $88 \pm 2$  mg per 100 ml in control animals (CTR)). As detailed elsewhere,<sup>3</sup> plasma insulin declined 50–33% over 2–30 days after the induction of diabetes. As shown in Table 1, weight reduction was noted over time, along with increasing kidney weight and kidney/body weight ratio. Marked polyuria developed, reflecting osmotic diuresis. This was associated with a rise in plasma urea (from  $7.0 \pm 0.2$  to  $16.9 \pm 5.3$  mmol l<sup>-1</sup>,  $P < 0.001$ ), whereas plasma creatinine was maintained, reflecting effective volume depletion. Creatinine clearance doubled over time (from  $0.41 \pm 0.02$  ml per min per 100 g in CTR to  $0.81 \pm 0.22$  ml per min per 100 g by day 30,  $P < 0.001$ ), and fractional sodium excretion increased from  $0.49 \pm 0.04$  to  $0.87 \pm 0.13\%$  ( $P < 0.05$ ).

Twenty-four hours following CM administration to diabetic rats, enhanced creatinine clearance declined by 45% (from  $0.83 \pm 0.04$  to  $0.45 \pm 0.08$  ml per min per 100 g,  $P < 0.001$ ), in association with enhanced medullary hypoxia and hypoxia adaptation. Nevertheless, renal structural integrity remained preserved.<sup>3</sup> In CTR animals given CM, renal structure was also intact and kidney function remained unaltered (creatinine clearance was  $0.37 \pm 0.05$  and  $0.39 \pm 0.03$  ml per min per 100 g before and after CM administration, respectively).<sup>3</sup>

### Kidney ECE protein and mRNA expression in STZ diabetic rats

Cortical ECE-1 protein remained largely unchanged following the induction of diabetes, increasing by 25% ( $P < 0.05$ ) only at 30 days (Figure 1a). By contrast, outer medullary ECE markedly increased at day 7 and thereafter, rising 5-fold by day 14 (Figure 1b) ( $P < 0.01$ ). The inner medulla exhibited an early effect, which was intermediate in extent, with ECE-1 protein increasing 50% after 2 days and reaching a maximal 2-fold increment by 7 days post-STZ (Figure 1c).

Intriguingly, unlike the changes in ECE-1 protein, ECE-1 mRNA levels in the outer medulla did not change over time ( $100 \pm 8$ ,  $86 \pm 20$ , and  $97 \pm 12\%$  at 7, 14, and 30 days of diabetes, respectively). Similarly, cortical ECE-1 mRNA was not altered either. By contrast, inner medullary ECE-1 mRNA gradually rose over time, reaching  $159 \pm 30$ ,  $233 \pm 25$ , and  $297 \pm 46\%$  of baseline, respectively ( $P < 0.05$  for the two longest time periods vs baseline). These observations suggest region-specific regulation pattern of ECE-1, potentially also reflecting different transcriptional and post-transcriptional mechanisms.

### Effect of contrast media on ECE-1 protein expression in control nondiabetic animals

In nondiabetic CTR rats, a 4-fold increase in ECE-1 protein expression was noted in the outer medulla 24 h after the administration of CM, as compared with nondiabetic animals not given CM (Figure 2b) ( $P < 0.01$ ). By contrast, in the cortex and inner medulla ECE protein remained unchanged (Figure 2a and c).

### Effect of contrast media on ECE-1 protein and mRNA expression in STZ diabetic rats

In diabetic animals (day 14), cortical ECE-1 protein remained unchanged as compared with CTR animals, but it

**Table 1 | Structural and functional changes in STZ diabetic rats along time**

Group (number of animals)	CTR (36)	D—2 days (8)	D—7 days (8)	D—14 days (35)	D—30 days (7)
Blood glucose at killing (mg per 100 ml)	$88 \pm 2$	$393 \pm 35^c$	$384 \pm 22^c$	$328 \pm 42^c$	$380 \pm 29^c$
Change in body weight (g)	Gain by $1-2$ g day <sup>-1</sup>	$-34 \pm 4$	$-44 \pm 8^a$	$-50 \pm 7^a$	$-104 \pm 8^c$
Final 2 kidney weight (g)	$3.06 \pm 0.10$	$3.27 \pm 0.31$	$2.91 \pm 0.10$	$3.63 \pm 0.17^b$	$3.66 \pm 0.35$
Final kidney/body weight ratio (%)	$0.84 \pm 0.02$	$0.99 \pm 0.04$	$1.04 \pm 0.04$	$1.22 \pm 0.05^c$	$1.58 \pm 0.07^c$
Urine volume (ml h <sup>-1</sup> )	$0.51 \pm 0.04$	ND	ND	$5.45 \pm 0.43^c$	$3.44 \pm 0.67^c$

ND, not determined; STZ, streptozotocin.

Control rats (CTR) are compared with diabetic animals (D) 2, 7, 14, and 30 days after the induction of diabetes. This table is modified from data extended from our previous publication, using the same animals for the evaluation of cellular hypoxia response.<sup>3</sup>

<sup>a</sup> $P < 0.05$ ; <sup>b</sup> $P < 0.01$ ; <sup>c</sup> $P < 0.001$  vs CTR animals, one-way analysis of variance.

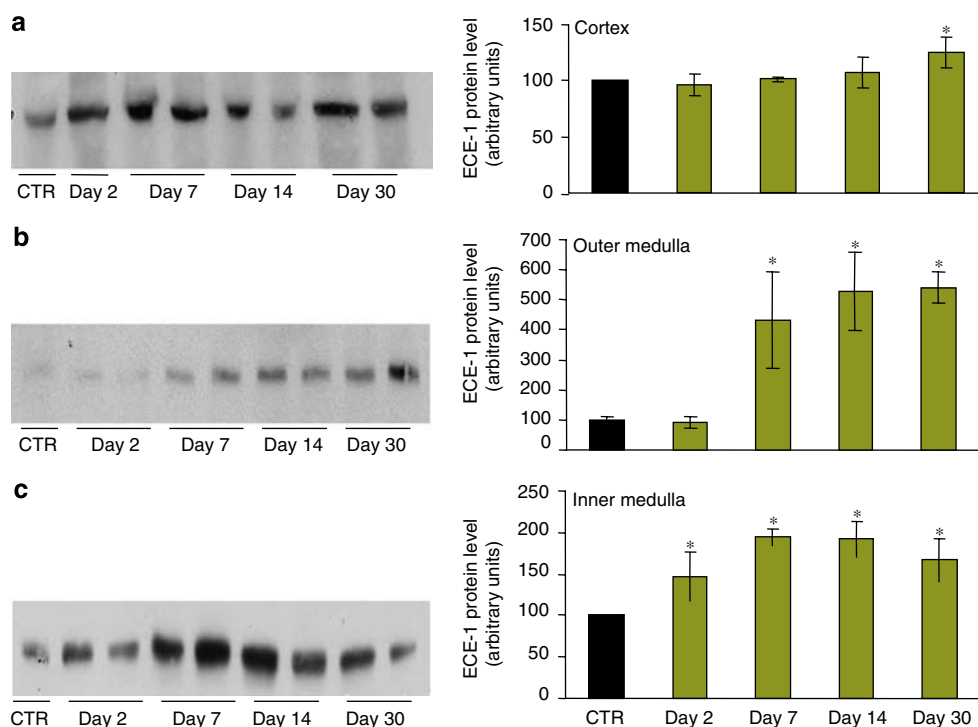


**Figure 1 | Time-dependent changes in ECE-1 protein following the induction of diabetes.** ECE-1 protein levels in kidney cortex (a), outer medulla (b), and inner medulla (c) as determined by western blot analysis. The right panels indicate the densitometric analysis for five animals in each group. CTR—control nondiabetic animals. D—diabetic. The duration of diabetes (days) is outlined on the x axis. Diabetes increased medullary ECE-1 protein expression over time. \* $P < 0.01$  compared with nondiabetic CTR animals.

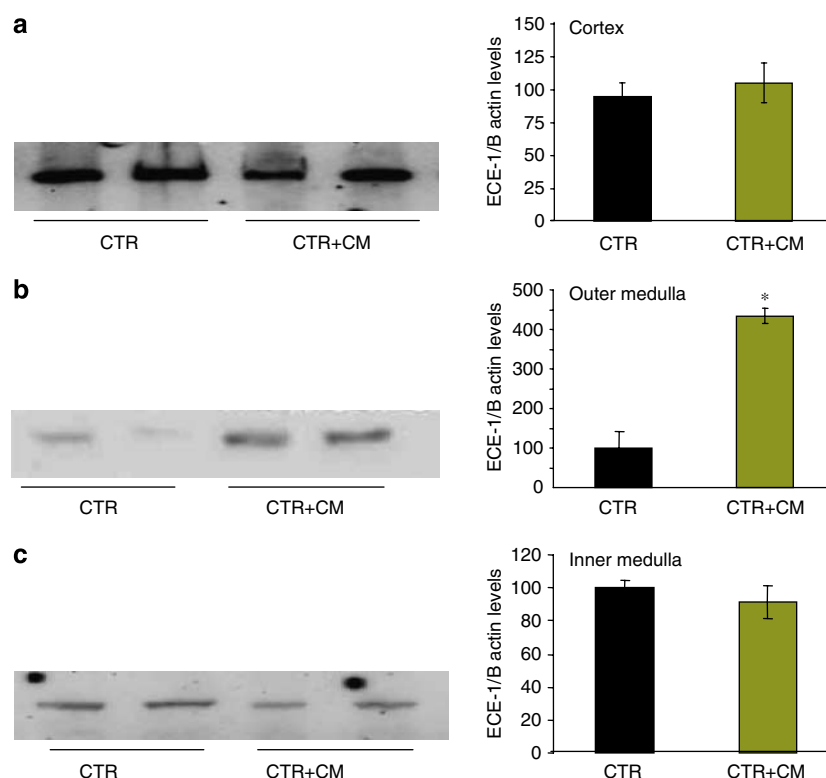


**Figure 2 | The effect of contrast media on ECE-1 protein.** ECE-1 protein levels in kidney cortex (a), outer medulla (b), and inner medulla (c) in nondiabetic control kidneys (CTR) and CTR infused with  $8 \text{ ml kg}^{-1}$  of 60% meglumine iohalamate (CTR + CM). The right panels indicate the densitometric analysis for five animals in each group. CM increased ECE-1 protein expression selectively in the outer medulla. \* $P < 0.01$  compared with nondiabetic CTR animals.

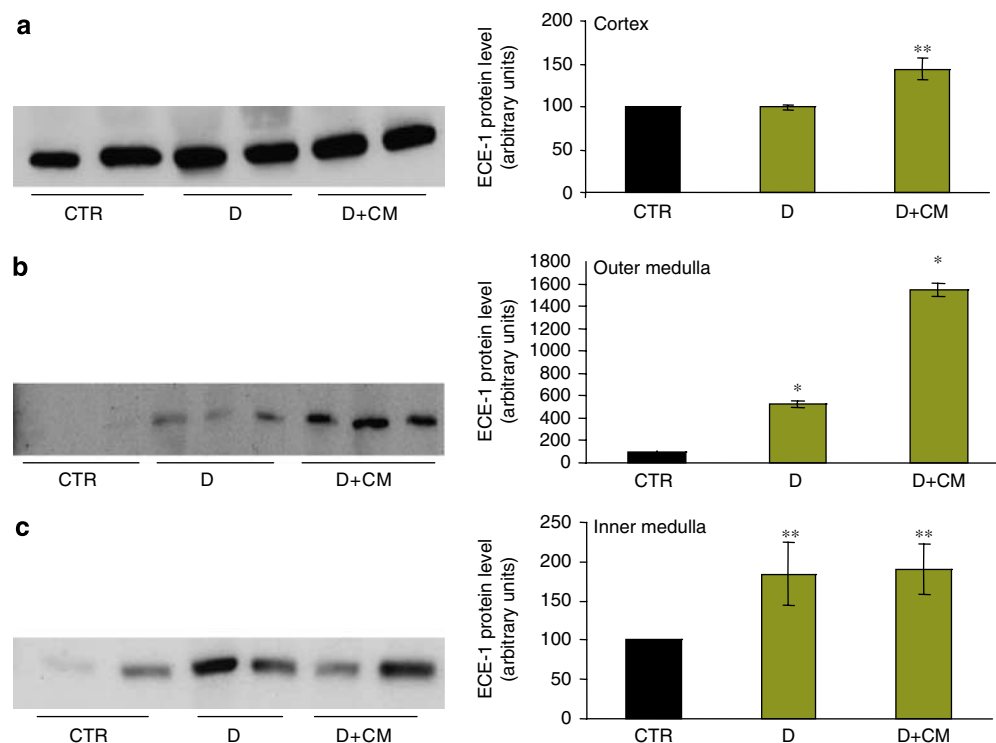


**Figure 3 | The effect of diabetes and contrast media on renal ECE-1 protein.** ECE-1 protein levels in kidney cortex (a), outer medulla (b), and inner medulla (c) in nondiabetic (CTR), 14 days diabetic (D), and 14 days diabetic animals infused with 8 ml kg<sup>-1</sup> of 60% meglumine iohalamate (D+CM). The right panels indicate the densitometric analysis for five animals in each group. Data are mean  $\pm$  s.e.m. Medullary ECE-1 protein increased in diabetic animals and were further augmented in the outer medulla and cortex following the administration of radiocontrast. \* $P < 0.001$  compared with nondiabetic CTR animals. \*\* $P < 0.01$  compared with nondiabetic CTR animals.

rose by 50% 24 h following the administration of CM ( $P < 0.01$ ) (Figure 3a). In the outer medulla, the 5-fold increase in ECE-1 protein levels associated with the induction of diabetes was further increased 3-fold 24 h after the administration of CM (altogether 15-fold increase vs CTR) (Figure 3b) ( $P < 0.001$ ). In the inner medulla, although ECE protein levels rose 2-fold in diabetic rats compared with CTR animals ( $P < 0.01$ ), CM did not elicit a further rise (Figure 3c). Changes in renal ECE-1 mRNA grossly paralleled alterations in the ECE-1 protein level, with outer medullary mRNA rising 2.9-fold 24 h following CM.

#### ECE-1 and endothelin ET<sub>B</sub> receptor expressions

Immunohistochemistry was applied to define the renal cell types expressing ECE-1. As shown in Figure 4, in the intact rat kidney, ECE-1 was widely expressed in tubular cells, principally in collecting ducts and medullary thick ascending limbs, and most prominently within the renal medulla. It was also expressed in glomerular podocytes and in vasa recta within the outer medulla.

As illustrated in Figure 5, although ET<sub>B</sub> immunostaining was faint at the outer medulla in CTR animals, in diabetic animals vasa recta and peritubular interstitial cells became strongly immunopositive in over 90% of samples at all time points throughout days 2–30 ( $n = 3–5$  for the different time points).

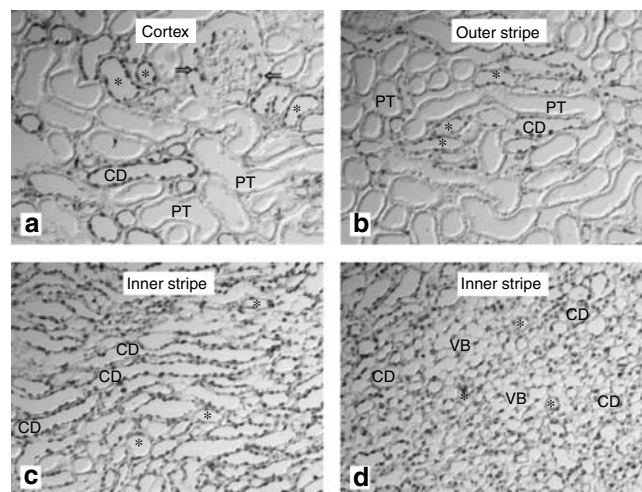


**Figure 4 | ECE-1 immunostaining in intact rat kidney.** ECE-1 protein immunostaining in CTR kidneys, with representing sections at the cortex (a), outer stripe (b), and inner stripe of the outer medulla (c—longitudinal section; d—tangential section). Arrow = glomerular cell, most likely podocyte; asterisk = either unspecified distal tubule in the cortical labyrinth or thick ascending limb in the medulla; CD = collecting duct; PT = proximal tubule; and VB = vascular bundle. PTs are all negative (a and b), whereas strong perinuclear signals appear in most CDs of all renal zones (a–d). Additional signals appear in glomeruli (a), in distal tubules (a–d), and in interstitial and/or endothelial cells of the medulla (c and d), including VBs (d). Original magnification  $\times 250$ .



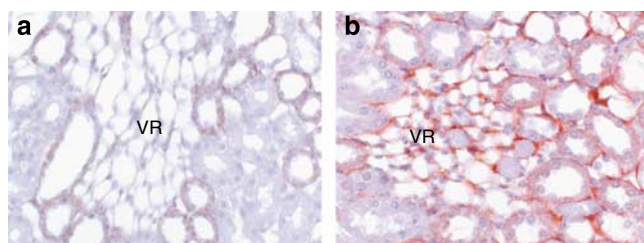


**Figure 5 | ET<sub>B</sub> immunostaining: the effect of diabetes.** ET<sub>B</sub> immunostaining of CTR (a) and 14-day STZ diabetic kidneys (b). These are horizontal cross-sections at the outermost level of the inner stripe of the outer medulla, illustrating vasa recta (vascular bundle, VB), surrounded by tubular components (medullary thick and thin limbs, and collecting ducts). Intense ET<sub>B</sub> immunostaining is noted in the diabetic kidney in vasa recta and peritubular vascular endothelial/interstitial cells. Original magnification  $\times 400$ .

### In vitro findings

Incubation of cultured endothelial cells at high glucose concentration significantly increased ET-1 levels already by 6 h (data not shown) reaching a 2.8-fold increase by 24 h (Figure 6). This was associated with a 30% increase in prepro-ET-1 mRNA at that time point (Figure 6). ECE-1 protein and mRNA levels were also raised by 70 and 20%, respectively (Figure 7).

Incubation with CM for 24 h also resulted in a 3-fold rise in ET-1, associated with a 45% increase in prepro-ET-1 mRNA. ECE-1 protein and mRNA rose 80 and 25%, respectively (Figures 6 and 7).

The increase in all the above parameters was generally more pronounced when cells were incubated for 24 h concomitantly at high glucose concentration, and with the presence of CM. ET-1 increased 4-fold, and ECE-1 protein and mRNA rose 220 and 45%, respectively. The rise in prepro-ET-1 (30%), however, was not further augmented by the addition of CM, and was identical to that observed with high glucose alone (Figures 6 and 7).

Noteworthy, increased medium osmolality by the addition of mannitol or hypertonic saline to levels comparable to the tested conditions of high glucose  $\pm$  CM did not exert a rise in ET-1 levels (data not shown), in agreement with previous reports,<sup>16,27</sup> suggesting a metabolic-mediated effect of glucose/CM, rather than the increase in osmolality *per se*.

In complementary studies, the direct impact of hypoxia upon ECE-1 was tested. Incubation of human vascular endothelial cells under hypoxic conditions resulted in a modest increase in cell death: the fractional released lactate dehydrogenase (LDH) activity over 24 h, expressed as the percentage of the total LDH activity, was  $10 \pm 4$  and  $22 \pm 6\%$  following normoxic and hypoxic incubations, respectively. Nevertheless, released ET-1 levels rose significantly, and ECE-1 protein expression increased (by 64 and 40%, respectively,  $P < 0.05$ ). In additional preliminary experiments, attenuation of oxidative stress by the addition of *N*-acetylcysteine ( $1 \text{ mmol l}^{-1}$ ), substantially blunted the increase in ET-1 levels and ECE-1 expression, invoked by high glucose concentration, by 62 and 48%, respectively ( $P < 0.05$ ).

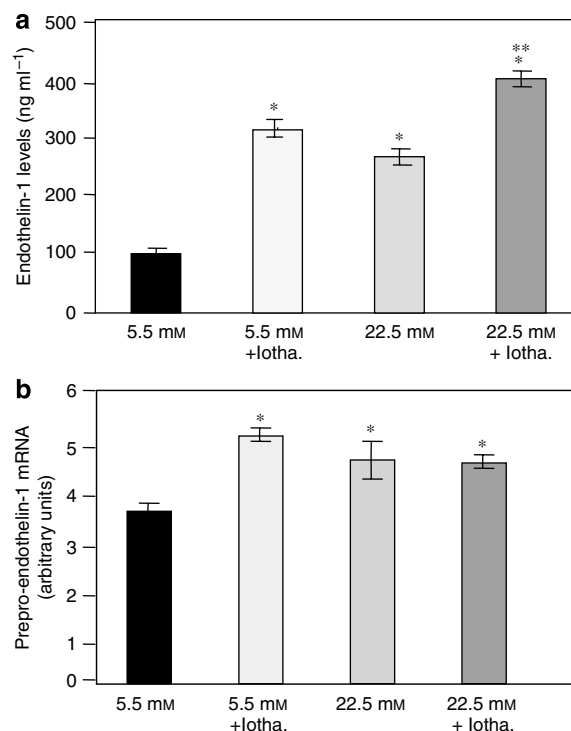


**Figure 6 | ET-1 and prepro-ET-1 expressions in culture endothelial cells.** ET-1 released into the culture medium (a) and prepro-ET-1 mRNA in cultured endothelial cells (b). Cells were incubated for 24 h with either 5.5 or 22.5 mmol l<sup>-1</sup> glucose, with or without concomitant exposure to meglumine iohalamate (9.7 mg per 100 ml iodine). Both ET-1 and prepro-ET-1 mRNA rose under hyperglycemic conditions and further increased with co-exposure to radiocontrast. Values represent the mean  $\pm$  s.d. of three experiments in triplicate. \* $P < 0.04$  compared with 5.5 mmol l<sup>-1</sup> glucose. \*\* $P < 0.03$  compared with 5.5 mmol l<sup>-1</sup> glucose, 22.5 mmol l<sup>-1</sup> glucose, and to 5.5 mmol l<sup>-1</sup> glucose + iohalamate.

### DISCUSSION

The formation of ET-1, the most prevalent biologically active member of the endothelin family, is initiated by furin-like enzymes, which cleave the pro-hormone (prepro-endothelin), and generate big endothelin. Subsequently, big endothelin undergoes a second proteolytic step by ECE isoforms and is cleaved into mature, active endothelins at the Trp21-Val/Ile22 bonds.<sup>24,28–31</sup>

Although most studies of endothelin induction focus on the generation of prepro endothelin data regarding the regulation of the final and perhaps critical step, namely ECE synthesis and activity are limited. Herein, we report increased ECE-1 expression in the renal parenchyma in diabetes and following CM administration. This increase most likely contributes to the elevated circulating and renal ET-1, reported in these two conditions.<sup>32,33</sup>

Of the two currently known ECE isoforms, ECE-1 has a broader tissue distribution, always expressed at higher levels than ECE-2 and has a central role in the endothelin system.<sup>34</sup> ECE-1 belongs to the neprilysin family of zinc metallo-peptidases,<sup>28,29</sup> and is abundantly expressed in the vascular

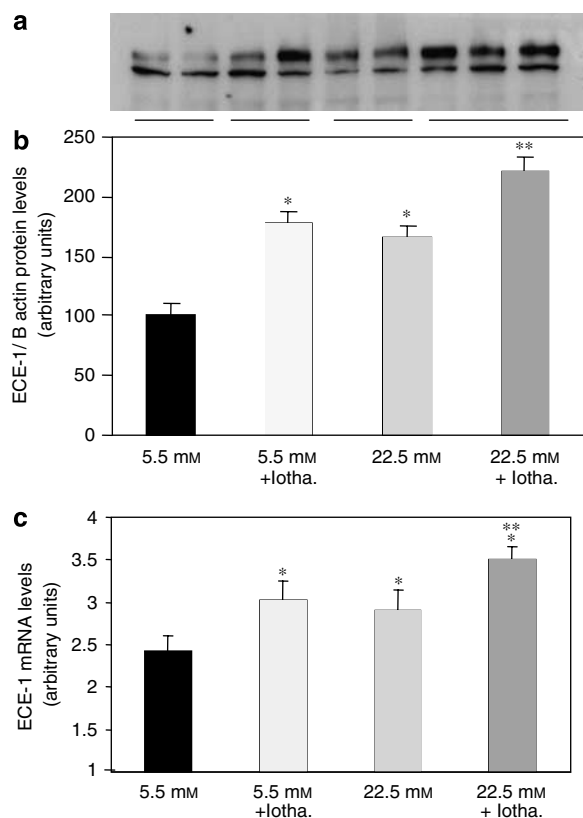


**Figure 7 | ECE-1 protein and mRNA in cultured endothelial cells.** ECE-1 protein densitometry (a), immunoblot (b), and mRNA (c) in cultured endothelial cells. Cells were incubated for 24 h with either 5.5 or 22.5 mmol l<sup>-1</sup> glucose, with or without concomitant exposure to meglumine iohalamate (9.7 mg per 100 ml iodine). Both ECE-1 protein and mRNA rose under hyperglycemic conditions and further increased with co-exposure to radiocontrast. Values represent the mean  $\pm$  s.d. of 2  $\times$  3 experiments in total. \* $P$  < 0.01 compared with 5.5 mmol l<sup>-1</sup> glucose. \*\* $P$  < 0.05 compared with 5.5 mmol l<sup>-1</sup> glucose, 22.5 mmol l<sup>-1</sup> glucose, and to 5.5 mmol l<sup>-1</sup> glucose + iohalamate.

endothelial cells of all tissues but is also found in nonvascular cells.<sup>35–39</sup> As a type II membrane protease, it is characterized by a single transmembrane region, a short NH<sub>2</sub>-terminal cytosolic tail, and a large COOH-terminal extracellular domain that contains the enzymatic active site.<sup>30</sup>

The potential role of ECE-1 in the regulation of endothelin synthesis has been explored in a few settings. *In vitro*, we have shown previously that ECE-1 protein and mRNA levels were elevated in endothelial cells incubated in high glucose media.<sup>27</sup> By contrast, ECE-1 mRNA expression in the renal cortex, medulla, and papilla was similar in Prague hypertensive rat and in normotensive counterpart.<sup>40</sup> High salt intake was reported to increase medullary ECE-1,<sup>41</sup> whereas experimental congestive heart failure stimulated cortical ECE-1 expression.<sup>42</sup> In rats acutely injected with cyclosporine A, an inverse association was found between ET-1 and ECE-1. Whereas prepro-ET-1 rapidly rose within 30–60 min, followed by an increase in plasma ET-1, ECE-1 mRNA was downregulated over 1–24 h in the glomeruli and along all nephron segments (both *in vivo* and *in vitro*), and ECE-1 protein levels declined in the outer and inner medulla

for as long as 96 h after exposure. ECE-1 mRNA recovered only 72 h after the administration of cyclosporine A.<sup>43</sup> The authors concluded that enhanced ET-1 levels following cyclosporine A exposure principally reflect upregulated prepro-ET-1 mRNA and synthesis, whereas glomerular and tubular ECE-1 (as well as ET receptor subtypes) is downregulated, perhaps as an adaptive response to enhanced ET synthesis.

Diabetes and radiocontrast agents are also associated with increased ET-1 levels, and ET-1 is believed to participate both in the pathogenesis of diabetic nephropathy<sup>44</sup> and in radiocontrast-induced acute renal dysfunction.<sup>45</sup> Interestingly, Clark *et al.*<sup>46</sup> found that ET-1 levels, already high at baseline, rose most pronouncedly in diabetic patients following radiocontrast studies. In the perspective of this observation, together with the peculiar susceptibility of diabetics to radiocontrast nephropathy it is tempting to assume that ET-1 has an important role in this disorder. Indeed, the administration of bosentan, a nonselective endothelin ET<sub>A</sub>/ET<sub>B</sub> receptor antagonist reduced albuminuria, increased glomerular filtration rate, and ameliorated mesangial matrix, fibronectin, and type IV collagen accumulation in diabetic rats.<sup>47</sup> Similarly, the selective inhibition of ET<sub>A</sub> receptors attenuates radiocontrast-induced medullary hypoxia<sup>48</sup> and has been suggested as a preventive measure against the development of contrast nephropathy in high-risk patients.<sup>49</sup>

Increased prepro-ET-1 mRNA was reported both in diabetes<sup>50</sup> and in cultured endothelial cells following the exposure to radiocontrast.<sup>51</sup> We also reported rising plasma ET-1 shortly after the administration of CM *in vivo*.<sup>16</sup> Our prepro-ET-1 findings *in vitro* are in accordance with these studies. The novel findings reported in the present series, both *in vivo* and *in vitro*, imply that increased ET-1 production in diabetes and following CM exposure may be mediated to a large extent by ECE-1 upregulation. Furthermore, the particularly pronounced upregulation of ECE-1 in diabetic animals following the administration of contrast medium, paralleling clinical evidence for highest ET-1 levels,<sup>46</sup> suggests a causal role for ECE-1/endothelin in contrast nephropathy, principally in the diabetic population. Further experiments, using knockout animals and selective ET-receptor antagonists are required to address this possibility.

The mechanisms controlling ECE-1 expression at various renal regions are yet to be defined. Our experiments *in vitro* indicate that the well-known upregulation of ET-1 under hypoxia<sup>52</sup> is associated with a parallel increase in ECE-1. Both experimental<sup>3</sup> and advanced human diabetes<sup>53</sup> are associated with renal parenchymal hypoxia, as also happen following radiocontrast administration,<sup>18</sup> particularly in the diabetic kidney.<sup>3</sup> Therefore, it is tempting to assume that hypoxia plays a role in the induction of ECE-1. Nevertheless, hypoxia may not be the sole mechanism, as we found ECE-1 induction by high glucose concentration or CM *in vitro* under normoxic conditions. Reactive oxygen species, generated in the diabetic kidney and following CM administration are additional potential mediators of ECE-1 upregulation. Our preliminary findings *in vitro*, showing attenuation of

ECE-1 upregulation with *N*-acetylcysteine support this possibility. However, so far reactive oxygen species were found to downregulate ECE-1 expression<sup>54</sup> and activity.<sup>55</sup> The intracellular mechanisms that lead to ECE induction are currently studied, and, apparently, ECE upregulation during hyperglycemia is mediated by protein-kinase C- $\delta$  (Khamaisi and Raz unpublished data).

Noteworthy, in our hands, ECE-1 protein levels and mRNA expression *in vivo* did not fully correspond, and were regulated in a region-specific manner. As mRNA measurements largely depend on quick tissue recovery and preservation, and in the presence of fully paralleled findings in cell cultures, this dys-synchrony *in vivo* conceivably reflects flawed tissue collection, particularly during the difficult time-consuming separation of the outer medulla. Alternatively, the dys-synchrony *in vivo* may reflect differences in the half-life of mRNA and the protein, or post-transcription mechanisms.

We also report the upregulation of ET<sub>B</sub> in vasa recta and peritubular capillaries in the outer medulla in STZ diabetic kidneys. Comparable pattern of ET<sub>B</sub> upregulation and distribution in the outer medullary microcirculation has previously been observed in animals with compensated heart failure<sup>25</sup> and following the induction of chronic tubulointerstitial disease, associated with medullary hypoxia.<sup>26</sup> The parallel expression of ECE-1 protein and ET<sub>B</sub> receptors in medullary vasa recta (Figures 4d and 5) conceivably reflects a local apocrine pattern of hormone function. Interestingly, although ET-1 is a most potent vasoconstrictor in most vascular beds, it induces selective outer medullary vasodilation, mediated by ET<sub>B</sub> receptors and nitric oxide.<sup>25,56</sup> We speculate that outer medullary ET<sub>B</sub> upregulation serves to maintain regional blood flow and oxygenation, as an adaptive response to increased endothelin concentrations and ambient hypoxia, noted in the diabetic kidney.<sup>3</sup> Indeed, severe hypertension and renal dysfunction develops in ET<sub>B</sub>-deficient diabetic rats.<sup>57</sup> In that respect, aggravation of contrast nephropathy in humans with the use of the nonselective ET<sub>A</sub>/ET<sub>B</sub> receptor antagonist bosentan<sup>58</sup> probably underscores the important role of ET<sub>B</sub> receptors in maintaining medullary oxygen sufficiency and integrity.<sup>59</sup>

In conclusion, evidence gathered so far suggests that ET-1 may be involved in the pathogenesis of chronic diabetes complications and in contrast nephropathy. Our findings imply that ECE-1 may play a key role in the upregulation of ET-1 levels under both circumstances, and propose an explanation for the particular susceptibility of diabetic patients to contrast media. In that perspective, ECE-1 may serve as a potential target for the development of new classes of drugs, designed for the prevention of diabetic complications and contrast nephropathy. Our findings and hypotheses should be further validated by clinical studies using ECE-1 inhibitors and ET receptor antagonists.

## MATERIALS AND METHODS

### Animals and materials

Male Sprague-Dawley rats 250–350 g were used, fed on regular chaw and given free excess to water. Experiments were conducted in

accord with the NIH Guide for the Care and Use of Laboratory Animals. Chemicals were purchased from Sigma (St Louis, MO, USA), if not stated otherwise. Rat anti-ECE-1 primary monoclonal antibody used for western blot analysis and immunohistochemistry was kindly received from Dr Rina Meidan (Rehovot, Israel). Anti-ET<sub>B</sub> primary monoclonal antibodies were obtained from Alomone Labs (Jerusalem, Israel), and the real-time PCR reagents were purchased from Agentek (Tel Aviv, Israel). LDH-L diagnostic reagent was purchased from Pointe Scientific Inc. (Canton, MI, USA).

### *In vivo* experiments

Diabetes was induced by intraperitoneal injection of freshly prepared STZ (65 mg per kg body weight, dissolved in 100 mmol l<sup>-1</sup> citric acid, pH 4.5), and confirmed 48 h later by blood glucose sampling from the tail tip.<sup>60</sup> Over 80% of injected animals were enrolled, with fed glucose levels >250 mg per 100 ml. The animals were kept two in a cage and studied 2, 7, 14, and 30 days later. Persistence of hyperglycemia was confirmed again before the animals were killed. Vehicle-injected animals served as controls.

In separate experiments, CTR and diabetic animals (14 days old) were infused with CM (8 ml kg<sup>-1</sup> of 60% meglumine iohalamate; Mallinckrodt, St Louis, MO, USA), and were killed 24 h later. Vehicle-injected animals served as controls. The 14-day time point was chosen as it yielded the most intense medullary hypoxia<sup>3</sup> and ECE-1 expression.

The animals fed on regular rat chaw and water *ad libitum*, were kept in metabolic cages (Nalge, Rochester, MD, USA) for urinary collection. Corresponding blood samples were obtained after the animals were killed. Kidney functional parameters were obtained and detailed in a previous publication, exploring renal hypoxia adaptation.<sup>3</sup> At the time indicated, animals were killed under anesthesia (pentobarbital, 60 mg kg<sup>-1</sup>). In some of the experiments, one or the two kidneys were perfusion fixed for morphology and immunohistochemistry. Non-perfusion-fixed kidneys were hastily removed, and rinsed in iced saline. Samples from the cortex, outer, and inner medulla (papilla) were collected, snap-frozen in liquid nitrogen, and kept in -70 °C until analyzed.

### *In vitro* studies

As vascular endothelial cells are the major source of endothelin synthesis, we used these cells to evaluate the isolated and independent effects of high glucose media and radioccontrast on the endothelin system. EA.hy926 cells, human umbilical vein endothelial cells fused with a human pulmonary epithelial cell line (A549), were cultured in Dulbecco's modified Eagle's medium as described by Waxman *et al.*<sup>61</sup> Cells were positively stained for von Willebrand factor using human anti-rabbit factor VIII antibody (Dako, Glostrup, Denmark).

For the experiments, cells were grown in 6-well plates conditioned with 5.5 mmol l<sup>-1</sup> glucose (CTR cell) and were compared with cells incubated at high glucose concentration (22.5 mmol l<sup>-1</sup>), with meglumine iohalamate (9.7 mg iodine per ml) or under the combined effect of high glucose and CM, for 1–24 h. Culture cell medium osmolarity was adjusted by adding mannitol or hypertonic saline to CTR cell culture. ET-1 levels were determined in the culture medium, while cells were used for the determination of prepro-ET-1 and ECE-1 protein and mRNA at the 24 h time point. ET-1 levels were determined using EIA kit (Cayman Chemical, Ann Arbor, MI, USA) in supernatants from different cell cultures as described before.<sup>62</sup>

For the hypoxic insult experiments, EA.hy926 cells, cultured in regular medium, were kept at 1% oxygen levels for 24 h, as described previously.<sup>63</sup> Oxygen tension was determined by an electronic oxygen sensor coupled to an oxygen monitor (Hudson RCI, Hanover, Germany). Cell death was measured at the end of the hypoxic insult by the release of LDH into the medium, as previously described.<sup>63</sup> ET-1 levels in supernatants were determined using EIA kit as described before.<sup>62</sup> Total cell lysate was used for determination of ECE-1 protein expression as described below.

### Western blot analysis for determination of ECE-1 protein expression

**In vitro.** At different time points, cells were washed with phosphate-buffered saline, lysed with lysis buffer (10 mmol l<sup>-1</sup> Tris, pH 7.4; 150 mmol l<sup>-1</sup> NaCl; and 1% NP-40) and centrifuged for 10 min at 10 000 r.p.m. at 4 °C. Supernatants were solubilized with SDS-polyacrylamide gel electrophoresis sample buffer.

**In vivo.** Total tissue lysate fractions were prepared from the cortex, the outer medulla, and the inner medulla of rat kidney as described previously.<sup>41</sup> Rats were killed at 2, 7, 14, and 30 days after the induction of diabetes. Kidneys were rapidly removed and transferred into phosphate-buffered saline on ice. Kidneys were sliced and separated into blocks of cortex, outer medulla, and inner medulla with a razor blade. Each part was minced and homogenized with five strokes at 1000 r.p.m., using a glass homogenizer, in lysis buffer (40 mmol l<sup>-1</sup> Tris-HCl, 20% glycerol, 500 mmol l<sup>-1</sup> NaCl, 6 mmol l<sup>-1</sup> ethylenediaminetetraacetic acid, 6 mmol l<sup>-1</sup> ethyleneglycol tetraacetate, 1% NP40, 2 mmol l<sup>-1</sup> *p*-nitrophenylphosphate, 40 mmol l<sup>-1</sup> β-glycerol phosphate, 1 mmol l<sup>-1</sup> NaVO<sub>4</sub>, 2 mol l<sup>-1</sup> dithiothreitol, 1 mmol l<sup>-1</sup> phenylmethylsulfonyl fluoride, 10 μg ml<sup>-1</sup> aprotinin, 10 μg ml<sup>-1</sup> leupeptin, pH 7.4) at 4 °C. The supernatant was collected after centrifugation at 10 000 r.p.m. for 15 min at 4 °C and stored at -70 °C until used. Protein concentrations were quantified using Bio-Rad protein assay reagent with bovine serum albumin as standard.

Total cell lysates (10 μg) or 75 μg of tissue protein lysate were electrophoretically fractionated on 7.5% SDS-polyacrylamide gel electrophoresis minigels and were electroblotted onto a nitrocellulose membrane. The membrane was sequentially incubated in TBS that contained 3% casein for 120 min and diluted (1:1000) bovine ECE-1 polyclonal antibody<sup>64</sup> in TBS for 12 h on a shaker at 4 °C. The blot was washed with TBS that contained 0.1% Tween-20 and was incubated with a 1:1000 dilution of horseradish peroxidase-conjugated goat anti-rabbit secondary antibody (Jackson ImmunoResearch Lab, West Grove, PA, USA) in TBS for 1 h at room temperature, washed with TBS, and incubated with the peroxidase substrate. Immunoreactive bands were visualized within 10 min using an ECL detection kit (Amersham Pharmacia Biotech, Piscataway, NJ, USA).<sup>65</sup>

### Real-time PCR for determination of ECE-1 and prepro-ET-1 mRNA expression

We used previously established semiquantitative real-time PCR assays<sup>66</sup> for ECE-1 expression. To monitor complementary DNA synthesis efficiency, glyceraldehyde-3-phosphate dehydrogenase was used as an internal CTR. As reported previously,<sup>41,34</sup> total RNA from the cells and kidney parts were extracted using the TRI Reagent according to the manufacturer's instructions. Complementary DNA was synthesized by reverse transcription of cellular RNA as previously described using the high capacity complementary DNA reverse transcription kits (Applied Biosystems, Foster City, CA,

USA). PCR primers for amplifying rat ECE-1 were selected from the rat gene sequence as previously reported.<sup>67</sup> The glyceraldehyde-3-phosphate dehydrogenase, ECE-1, and prepro-ET-1 complementary DNA were PCR amplified using primers obtained from Agentek. ECE-1 sequence was PCR amplified using a similar procedure except that the number of cycles was increased to 30 and the annealing temperature was increased to 58 °C. A dissociation curve analysis was run after each real-time experiment to confirm the presence of only one product and the absence of formation of primer dimers. The threshold cycle number (C<sub>t</sub>) for each tested gene X was used to quantify the relative abundance of the gene:  $2^{-(C_t \text{ gene X} - C_t \text{ G3PDH})} \times 1000$ .

### Endothelin ET<sub>B</sub> receptor immunohistochemistry

As we have previously reported upregulation of renal medullary endothelin ET<sub>B</sub> receptors under conditions threatening medullary oxygen sufficiency,<sup>25,26</sup> we complemented these series by looking at the effect of diabetes upon renal endothelin ET<sub>B</sub> expression. CTR and diabetic kidneys (2–30 days) were perfusion fixed with paraformaldehyde through the abdominal aorta, stored in ice-cooled phosphate-buffered saline, and processed for paraffin embedding as previously detailed.<sup>3</sup> Three-micron paraffin sections were processed for routine histology and immunohistochemistry. Hematoxylin and eosin staining was performed according to standard procedures. Immunohistochemistry was carried out using the anti-ET<sub>B</sub> primary monoclonal antibodies (1:200).

### ECE-1 immunohistochemistry

As paraffin sections proved inappropriate for this staining—despite of antigen retrieval techniques like cooking or proteinase digestion—we employed 5 μm cryostat sections. To avoid freezing artifacts, perfusion-fixed kidneys were kept for 2 h in 800 mosmol l<sup>-1</sup> sucrose in phosphate-buffered saline (pH 7.4, 4 °C), after which they were snap-frozen in isopentane cooled by liquid nitrogen. Immunohistochemistry was carried out with the help of a catalyzed signal amplification (CSA) kit from Dako (Hamburg, Germany) using rabbit-anti ECE-1 antibody (1:10 000).

### Statistics

Data are represented as means ± s.d. Student's *t*-test and multiple comparisons with *T*-test *post hoc* analysis of variance were used as indicated below for the comparison of protein and mRNA parameters. Statistical significance was set at *P* < 0.05.

### ACKNOWLEDGMENTS

This work was supported by the Russell Berrie Foundation and D-Cure, Diabetes Care in Israel.

### REFERENCES

1. Palm F, Cederberg J, Hansell P et al. Reactive oxygen species cause diabetes-induced decrease in renal oxygen tension. *Diabetologia* 2003; **46**: 1153–1160.
2. Ries M, Basseau F, Tyndal B et al. Renal diffusion and BOLD MRI in experimental diabetic nephropathy. Blood oxygen level-dependent. *J Magn Reson Imaging* 2003; **17**: 104–113.
3. Rosenberger C, Khamaisi M, Abassi Z et al. Adaptation to hypoxia in the diabetic rat kidney. *Kidney Int* 2008; **73**: 34–42.
4. Brezis M, Rosen S. Hypoxia of the renal medulla—its implications for disease. *N Engl J Med* 1995; **332**: 647–655.
5. Scherzer P, Nachliel I, Bar-On H et al. Renal Na-K-ATPase hyperactivity in diabetic *Psammomys obesus* is related to glomerular hyperfiltration but is insulin-independent. *J Endocrinol* 2000; **167**: 347–354.
6. Palm F. Intrarenal oxygen in diabetes and a possible link to diabetic nephropathy. *Clin Exp Pharmacol Physiol* 2006; **33**: 997–1001.



7. Leon CA, Raji L. Interaction of haemodynamic and metabolic pathways in the genesis of diabetic nephropathy. *J Hypertens* 2005; **23**: 1931–1937.
8. Li B, Yao J, Kawamura K et al. Real-time observation of glomerular hemodynamic changes in diabetic rats: effects of insulin and ARB. *Kidney Int* 2004; **66**: 1939–1948.
9. Klahr S, Morrissey J. Arginine as a therapeutic tool in kidney disease. *Semin Nephrol* 2004; **24**: 389–394.
10. Nishiyama A, Miyatake A, Aki Y et al. Adenosine A(1) receptor antagonist KW-3902 prevents hypoxia-induced renal vasoconstriction. *J Pharmacol Exp Ther* 1999; **291**: 988–993.
11. Nangaku M. Chronic hypoxia and tubulointerstitial injury: a final common pathway to end-stage renal failure. *J Am Soc Nephrol* 2006; **17**: 17–25.
12. VanZee BE, Hoy WE, Talley TE et al. Renal injury associated with intravenous pyelography in nondiabetic and diabetic patients. *Ann Intern Med* 1978; **89**: 51–54.
13. Barshay ME, Kaye JH, Goldman R et al. Acute renal failure in diabetic patients after intravenous infusion pyelography. *Clin Nephrol* 1973; **1**: 35–39.
14. Rudnick MR, Goldfarb S, Wexler L et al. Nephrotoxicity of ionic and nonionic contrast media in 1196 patients: a randomized trial. The Iohexol Cooperative Study. *Kidney Int* 1995; **47**: 254–261.
15. McCullough PA, Wolyn R, Rocher LL et al. Acute renal failure after coronary intervention: incidence, risk factors, and relationship to mortality. *Am J Med* 1997; **103**: 368–375.
16. Heyman SN, Clark BA, Kaiser N et al. Radiocontrast agents induce endothelin release *in vivo* and *in vitro*. *J Am Soc Nephrol* 1992; **3**: 58–65.
17. Rosenberger C, Heyman SN, Rosen S et al. Upregulation of HIF in acute renal failure: evidence for a protective transcriptional response to hypoxia. *Kidney Int* 2005; **67**: 531–542.
18. Heyman SN, Rosen S, Rosenberger C. Renal parenchymal hypoxia, hypoxia adaptation, and the pathogenesis of radiocontrast nephropathy. *Clin J Am Soc Nephrol* 2008; **3**: 288–296.
19. Khan ZA, Farhangkhoei H, Mahon JL et al. Endothelins: regulators of extracellular matrix protein production in diabetes. *Exp Biol Med (Maywood)* 2006; **231**: 1022–1029.
20. Itoh Y, Nakai A, Kakizawa H et al. Alteration of endothelin-1 concentration in STZ-induced diabetic rat nephropathy. Effects of a PGI(2) derivative. *Horm Res* 2001; **56**: 165–171.
21. Kohan DE. The renal medullary endothelin system in control of sodium and water excretion and systemic blood pressure. *Curr Opin Nephrol Hypertens* 2006; **15**: 34–40.
22. Oldroyd S, Slee SJ, Haylor J et al. Role for endothelin in the renal responses to radiocontrast media in the rat. *Clin Sci (Lond)* 1994; **87**: 427–434.
23. Attina T, Camidge R, Newby DE et al. Endothelin antagonism in pulmonary hypertension, heart failure, and beyond. *Heart* 2005; **6**: 825–831.
24. Davenport AP, Maguire JJ. Endothelin. *Handb Exp Pharmacol* 2006; **176**(Part 1): 295–329.
25. Francis BN, Abassi Z, Heyman S. Differential regulation of ET<sub>A</sub> and ET<sub>B</sub> in the renal tissue of rats with compensated and decompensated heart failure. *J Cardiovasc Pharmacol* 2004; **44**: S362–S365.
26. Goldfarb M, Rosenberger C, Abassi Z et al. Acute-on-chronic renal failure in the rat: functional compensation and hypoxia tolerance. *Am J Nephrol* 2006; **26**: 22–33.
27. Keyman S, Khamaisi M, Dahan R et al. Increased expression of endothelin-converting enzyme-1c isoform in response to high glucose levels in endothelial cells. *J Vasc Res* 2004; **41**: 131–140.
28. Xu D, Emoto N, Giaid A et al. ECE-1: a membrane-bound metalloprotease that catalyzes the proteolytic activation of big endothelin-1. *Cell* 1994; **78**: 473–485.
29. Valdenaire O, Schweizer A. Endothelin-converting enzyme-like 1 (ECE1; 'XCE'): a putative metallopeptidase crucially involved in the nervous control of respiration. *Biochem Soc Trans* 2000; **28**: 426–430.
30. Schmidt M, Kroger B, Jacob E et al. Molecular characterization of human and bovine endothelin converting enzyme (ECE-1). *FEBS Lett* 1994; **356**: 238–243.
31. Turner AJ, Barnes K, Schweizer A et al. Isoforms of endothelin-converting enzyme: why and where? *Trends Pharmacol Sci* 1998; **19**: 483–486.
32. Itoh Y, Nakai A, Kakizawa H et al. Alteration of endothelin-1 concentration in STZ-induced diabetic rat nephropathy. Effects of a PGI(2) derivative. *Horm Res* 2001; **56**: 165–171.
33. Persson PB, Tepel M. Contrast medium-induced nephropathy: the pathophysiology. *Kidney Int Suppl* 2006; **100**: S8–S10.
34. Muller L, Barret A, Etienne E et al. Heterodimerization of endothelin-converting enzyme-1 isoforms regulates the subcellular distribution of this metalloprotease. *J Biol Chem* 2003; **278**: 545–555.
35. Boussette N, Giaid A. Endothelin-1 in atherosclerosis and other vasculopathies. *Can J Physiol Pharmacol* 2003; **81**: 578–587.
36. Maguire JJ, Johnson CM, Mockridge JW et al. Endothelin converting enzyme (ECE) activity in human vascular smooth muscle. *Br J Pharmacol* 1997; **122**: 1647–1654.
37. Sawamura T, Shinmi O, Kishi N et al. Characterization of phosphoramidon-sensitive metalloproteinases with endothelin-converting enzyme activity in porcine lung membrane. *Biochim Biophys Acta* 1993; **1161**: 295–302.
38. Levy N, Gordin M, Smith MF et al. Hormonal regulation and cell-specific expression of endothelin-converting enzyme 1 isoforms in bovine ovarian endothelial and steroidogenic cells. *Biol Reprod* 2003; **68**: 1361–1368.
39. Korth P, Bohle RM, Corvol P et al. Cellular distribution of endothelin-converting enzyme-1 in human tissues. *J Histochem Cytochem* 1999; **47**: 447–462.
40. Vogel V, Backer A, Heller J et al. The renal endothelin system in the Prague hypertensive rat, a new model of spontaneous hypertension. *Clin Sci (Lond)* 1999; **97**: 91–98.
41. Fattal I, Abassi Z, Ovcharenko E et al. Effect of dietary sodium intake on the expression of endothelin. *Nephron Physiol* 2004; **98**: p89–p96.
42. Abassi Z, Winaver J, Rubinstein I et al. Renal endothelin-converting enzyme in rats with congestive heart failure. *J Cardiovasc Pharmacol* 1998; **31**(Suppl 1): S31–S34.
43. Nakayama Y, Nonoguchi H, Kiyama S et al. Intranephron distribution and regulation of endothelin-converting enzyme-1 in cyclosporin A-induced acute renal failure in rats. *J Am Soc Nephrol* 1999; **10**: 562–571.
44. Sarafidis PA, Ruilope LM. Insulin resistance, hyperinsulinemia, and renal injury: mechanisms and implications. *Am J Nephrol* 2006; **26**: 232–244.
45. Persson B. Contrast-induced nephropathy. *Eur Radiol* 2005; **15**(Suppl 4): D65–D69.
46. Clark BA, Kim D, Epstein FH. Endothelin and atrial natriuretic peptide levels following radiocontrast exposure in humans. *Am J Kidney Dis* 1997; **30**: 82–86.
47. Sorokin A, Kohan DE. Physiology and pathology of endothelin-1 in renal mesangium. *Am J Physiol Renal Physiol* 2003; **285**: F579–F589.
48. Liss P, Carlsson PO, Nygren A et al. ET-A receptor antagonist BQ123 prevents radiocontrast media-induced renal medullary hypoxia. *Acta Radiol* 2003; **44**: 111–117.
49. Pollock DM, Polakowski JS, Wegner CD et al. Beneficial effect of ETA receptor blockade in a rat model of radiocontrast-induced nephropathy. *Ren Fail* 1997; **19**: 753–761.
50. Takagi C, Bursell SE, Lin YW et al. Regulation of retinal hemodynamics in diabetic rats by increased expression and action of endothelin-1. *Invest Ophthalmol Vis Sci* 1996; **37**: 2504–2518.
51. Cantley LG, Heyman SN, Epstein FH. Radiocontrast agents induce endothelin-1 mRNA in bovine endothelial cells. *J Am Soc Nephrol* 1991; **2**: 660 (Abstract).
52. Kourembanas S, Marsden PA, McQuillan LP et al. Hypoxia induces endothelin gene expression and secretion in cultured human endothelium. *J Clin Invest* 1991; **88**: 1054–1057.
53. Haase VH. Hypoxia-inducible factors in the kidney. *Am J Physiol Renal Physiol* 2006; **291**: F271–F281.
54. Masatsugu K, Itoh H, Chun TH et al. Shear stress attenuates endothelin and endothelin-converting enzyme expression through oxidative stress. *Regul Pept* 2003; **111**: 13–19.
55. López-Ongil S, Senchak V, Saura M et al. Superoxide regulation of endothelin-converting enzyme. *J Biol Chem* 2000; **275**: 26423–26427.
56. Heyman SN, Goldfarb M, Darmon D et al. Tissue oxygenation modifies nitric oxide bioavailability. *Microcirculation* 1999; **6**: 199–203.
57. Pfab T, Thöne-Reineke C, Theilig F et al. Diabetic endothelin B receptor-deficient rats develop severe hypertension and progressive renal failure. *J Am Soc Nephrol* 2006; **17**: 1082–1089.
58. Wang A, Holcslaw T, Bashore TM et al. Exacerbation of radiocontrast nephrotoxicity by endothelin receptor antagonism. *Kidney Int* 2000; **57**: 1675–1680.
59. Heyman SN, Rosenberger C, Rosen S. Regional alterations in renal hemodynamics and oxygenation: a role in radiocontrast nephropathy. *Nephrol Dial Transplant* 2005; **20**(Suppl 1): i6–i11.
60. Khamaisi M, Rudich A, Beerl I et al. Metabolic effects of gamma-linolenic acid-alpha-lipoic acid conjugate in streptozotocin diabetic rats. *Antioxid Redox Signal* 1999; **1**: 523–535.
61. Waxman L, Doshi KP, Gaul SL et al. Identification and characterization of endothelin converting activity from EAHY 926 cells: evidence for the

- physiologically relevant human enzyme. *Arch Biochem Biophys* 1994; **308**: 240–253.
62. Santaniello A, Salazar G, Lenna S *et al.* HLA-B35 upregulates the production of endothelin-1 in HLA-transfected cells: a possible pathogenetic role in pulmonary hypertension. *Tissue Antigens* 2006; **68**: 239–244.
63. Tabakman R, Lazarovici P, Kohen R. Neuroprotective effects of carnosine and homocarnosine on pheochromocytoma PC12 cells exposed to ischemia. *J Neurosci Res* 2002; **68**: 463–469.
64. Meidan R, Klipper E, Gilboa T *et al.* Endothelin-converting enzyme-1, abundance of isoforms a–d and identification of a novel alternatively spliced variant lacking a transmembrane domain. *J Biol Chem* 2005; **280**: 40867–40874.
65. Khamaisi M, Keynan S, Bursztyn M *et al.* Role of renal nitric oxide synthase in diabetic kidney disease during the chronic phase of diabetes. *Nephron Physiol* 2006; **102**: p72–p80.
66. Terada Y, Moriyama T, Martin BM *et al.* RT-PCR microlocalization of mRNA for guanylyl cyclase-coupled ANF receptor in rat kidney. *Am J Physiol* 1991; **261**(6 Part 2): F1080–F1087.
67. Sakurai T, Yanagisawa M, Takawa Y *et al.* Cloning of a cDNA encoding a non-isopeptide-selective subtype of the endothelin receptor. *Nature* 1990; **348**: 732–735.